research

report

PRESSURE RESPONSE IN A LONG TUBE
WHICH IS CLOSED AT ONE END

M. D. Bennett, 7131-1

November 1961
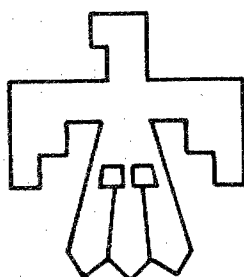
Sandia Corporation

CONTRACTOR FOR U. S. ATOMIC ENERGY COMMISSION

SC-4646(RR)

PRESSURE RESPONSE IN A LONG TUBE
WHICH IS CLOSED AT ONE END

by

M. D. Bennett, 7131-1

November 1961

ABSTRACT

An equation is derived that approximately describes pressure re-
sponse in a long constant-diameter tube which is closed at one of its ex-
tremities. Numerical solutions are presented for several types of forc-
ing functions.

TABLE OF CONTENTS

LIST OF ILLUSTRATIONS

LIST OF SYMBOLS

A   constant for ramp function

C   atmospheric constant

C_P pressure coefficient, $(p - p_\infty)/q_\infty$

d   tube diameter

F   body force per unit volume or function

g   acceleration due to gravity

h   altitude

h*   reference altitude

k   Boltzmann's constant

K   parameter, $(p_o t^* d^2)/(64\mu L^2)$

ℓ length required to attain fully developed velocity profile

L   tube length

M   Mach number

n   constant

p   static pressure

p_o reference pressure (see "Results" section)

P   pressure coefficient, p/p_o

q   free-stream dynamic pressure

r   tube radial coordinate

r_o tube radius

R   universal gas constant

R_N Reynolds number

t   time

t*   interval of time

T   temperature

v   gas velocity

$\overline{V}$ constant flight velocity

x   tube axial coordinate or axis

X   dimensionless coordinate, x/L

Z   gas compressibility factor

γ ratio of specific heats

λ mean-free path

μ coefficient of gas viscosity

ξ dimensionless constant

ρ gas density

σ molecule radius

τ dimensionless time, t/t^*

ϕ flight path angle with respect to horizontal plane

ψ angle of tube longitudinal axis with respect to horizontal plane

Subscripts

o   reference

1   open end of tube

2   closed end of tube

∞ ambient or free-stream

a   apparent

r   radial

x   axial

X   derivative with respect for tube axial coordinate x/L

θ tangential

$\dot{}$ derivative with respect to time t/t^*

SUMMARY

An analysis is made of pressure response in a system that consists of a tube open at one extremity and terminating at the other end in a reservoir. The analysis concerns the continuum regime and pertains to fully developed laminar flow of a compressible fluid with isothermal state changes. An equation is derived that approximately describes pressure response in the system when the tube is long and the reservoir volume is small. The response equation is made dimensionless, and numerical solutions are presented for three types of boundary conditions: step functions, ramp functions, and the functions dictated by constant-velocity flight in an isothermal atmosphere. The results of this analysis may be used to determine response in pressure-sensing systems during the transient conditions of flight in real atmospheres, and in systems subjected to impulse pressure functions.

ACKNOWLEDGMENT

6

PRESSURE RESPONSE IN A LONG TUBE
WHICH IS CLOSED AT ONE END

Introduction

It is often necessary to measure a thermodynamic property such as pressure or density during transient conditions. A typical sensing system may consist of a tube which is joined at one extremity to an orifice and is connected at the other end to a reservoir that has an element suitable for measurement of the thermodynamic property. If the tube is long or the reservoir volume is large, the measured value may be significantly different from the value applied at the orifice, particularly when the pressure is low. To interpret that type of measurement or to design sensing systems, the response characteristics of the system must be established.

Vaughn (see Bibliography) derives an equation that describes pressure response in a reservoir with a tube of negligible length. Vaughn's equation, which is nonlinear, permits a more accurate estimate of pressure response than the linear treatment that makes use of a time constant. Ducoffe and White (see Bibliography) present an analytical and experimental study of pressure response in a sensing system which has a long tube and a reservoir of finite volume. Ducoffe's study considers typical missile sensing systems which are subjected to both impulse and continuous transient input pressure functions. These two studies are concerned with the continuum flow regime. Pressure response at extremely low pressure where slip and molecular flows occur is discussed in Davis (see Bibliography).

The analysis presented here concerns the pressure response in a sensing system which consists of a long tube connected to a negligible-volume reservoir. This system may be represented simply by a tube or duct which is closed at one of its extremities. An equation is derived that approximately describes pressure response in laminar flows of a compressible fluid in a constant-diameter tube. The analysis makes use of the Poiseuille equation for laminar flow with isothermal state changes. A common derivation of this equation is included, and the assumptions and limitations in the analysis are discussed with reference to the conditions encountered during flight through the earth's atmosphere. Numerical solutions of the equation are obtained for three types of boundary conditions: step functions, ramp (linear) functions, and the functions that represent constant-velocity flight--both ascent and descent--in an isothermal atmosphere.

The first two types of functions may be used with systems subjected to impulse pressure functions such as blast waves or shock waves. The last type may be used to determine pressure response during variable-velocity flight in real atmospheres.

Analysis

The equation of continuity may be derived from the law of conservation of mass using the concept of a continuum. This concept is applicable when the mean-free path λ of the fluid molecules is small compared with the smallest significant dimension in the problem; i.e., the tube diameter d in the present study. Since the

mean-free path in the earth's atmosphere is less than 2×10^{-4} inches at altitudes up to 10^5 feet, the continuity equation based on the concept of a continuous fluid is valid up to high altitudes for measuring systems of general concern. In cylindrical coordinates, the equation of continuity of a compressible fluid is

$$\frac{\partial \rho}{\partial t} + \left(\frac{1}{r}\right)\frac{\partial \rho v_r}{\partial r} + \left(\frac{1}{r}\right)\frac{\partial \rho v_\theta}{\partial \theta} + \frac{\partial \rho v_x}{\partial x} = 0 , \tag{1}$$

where

ρ is fluid density

t is time, and

v_r, v_θ, and v_x are the radial, tangential, and axial velocity components with respect to the tube along the directions r, θ, and x, respectively.

The equation of state of a gas is

$$\rho = \frac{p}{ZRT} , \tag{2}$$

where, in general, the dimensionless compressibility factor $Z = Z(p, t)$. By substituting Equation 2 into Equation 1 and by assuming a perfect gas (Z = constant), the following equation is obtained

$$\frac{\partial p}{\partial t} - \left(\frac{p}{T}\right)\frac{\partial T}{\partial t} + v_r\frac{\partial p}{\partial r} - \left(\frac{p v_r}{T}\right)\frac{\partial T}{\partial r} + p\frac{\partial v_r}{\partial r} + \left(\frac{v_\theta}{r}\right)\frac{\partial p}{\partial \theta} - \left(\frac{p v_\theta}{rT}\right)\frac{\partial T}{\partial \theta} + \left(\frac{p}{r}\right)\frac{\partial v_\theta}{\partial \theta} + v_x\frac{\partial p}{\partial x} - \left(\frac{p v_x}{T}\right)\frac{\partial T}{\partial x} +$$

$$p\frac{\partial v_x}{\partial x} + \frac{p v_r}{r} = 0 . \tag{3}$$

With air at sea-level pressure, Z is constant within 1/2 percent over the temperature interval $-100^\circ < T < 4400^\circ$F, and, at a pressure of 10^{-2} atmospheres, Z varies about 1/2 percent over the interval $-300^\circ < T < 3600^\circ$F. Thus, over a broad range of thermodynamic conditions, no large variations occur in the compressibility factor.

The equations of motion (Navier-Stokes equations) are derived from Newton's second law and Stokes law of friction. In the derivation of Stokes law, the assumption is made that fluid stresses are proportional to the rate of change of strain with time. This assumption is valid for laminar flow only. Although laminar flow has been maintained to Reynolds numbers as large as 20,000 by minimizing flow disturbance at the tube inlet, experiments have shown that steady flow in a tube is normally laminar at Reynolds numbers up to approximately 2000. Further, experiments have shown that the motion is stable in laminar flow--i.e., an initially turbulent flow will not be maintained indefinitely. The three equations of motion of a compressible, viscous fluid are

$$\rho\left[\frac{\partial v_r}{\partial t} + (v_r)\frac{\partial v_r}{\partial r} + \left(\frac{v_\theta}{r}\right)\frac{\partial v_r}{\partial \theta} + (v_x)\frac{\partial v_r}{\partial x} - \frac{v_\theta^2}{r}\right] = F_r - \frac{\partial p}{\partial r} + \frac{\partial}{\partial r}\left\{\mu\left[2\frac{\partial v_r}{\partial r} - \left(\frac{2}{3}\right)\operatorname{div}\vec{v}_v\right]\right\} +$$

$$\left(\frac{1}{r}\right)\frac{\partial}{\partial \theta}\left\{\mu\left[\left(\frac{1}{r}\right)\frac{\partial v_r}{\partial \theta} + \frac{\partial v_\theta}{\partial r} - \frac{v_\theta}{r}\right]\right\} + \frac{\partial}{\partial x}\left[\mu\left(\frac{\partial v_r}{\partial x} + \frac{\partial v_x}{\partial r}\right)\right] + 2\left(\frac{\mu}{r}\right)\left[\frac{\partial v_r}{\partial r} - \left(\frac{1}{r}\right)\frac{\partial v_\theta}{\partial \theta} - \frac{v_r}{r}\right] , \tag{4}$$

$$\rho\left[\frac{\partial v_\theta}{\partial t} + (v_r)\frac{\partial v_\theta}{\partial r} + \left(\frac{v_\theta}{r}\right)\frac{\partial v_\theta}{\partial \theta} + (v_x)\frac{\partial v_\theta}{\partial x} + \frac{v_r v_\theta}{r}\right] = F_\theta - \left(\frac{1}{r}\right)\frac{\partial p}{\partial \theta} + \left(\frac{1}{r}\right)\frac{\partial}{\partial \theta}\left\{\mu\left[\left(\frac{2}{r}\right)\frac{\partial v_\theta}{\partial \theta} - \left(\frac{2}{3}\right)\operatorname{div}\vec{v}_v\right]\right\} +$$

$$\frac{\partial}{\partial x}\left\{\mu\left[\frac{1}{r}\frac{\partial v_x}{\partial \theta} + \frac{\partial v_\theta}{\partial x}\right]\right\} + \frac{\partial}{\partial r}\left\{\mu\left[\left(\frac{1}{r}\right)\frac{\partial v_r}{\partial \theta} + \frac{\partial v_\theta}{\partial r} - \frac{v_\theta}{r}\right]\right\} + \left(\frac{2\mu}{r}\right)\left[\left(\frac{1}{r}\right)\frac{\partial v_r}{\partial \theta} + \frac{\partial v_\theta}{\partial r} - \frac{v_\theta}{r}\right] , \qquad (5)$$

$$\rho\left[\frac{\partial v_x}{\partial t} + (v_r)\frac{\partial v_x}{\partial r} + \left(\frac{v_\theta}{r}\right)\frac{\partial v_x}{\partial \theta} + (v_x)\frac{\partial v_x}{\partial x}\right] = F_x - \frac{\partial p}{\partial x} + \frac{\partial}{\partial x}\left\{\mu\left[2\frac{\partial v_x}{\partial x} - \left(\frac{2}{3}\right)\operatorname{div}\vec{v}_v\right]\right\} +$$

$$\left(\frac{1}{r}\right)\frac{\partial}{\partial r}\left[\mu r\left(\frac{\partial v_r}{\partial x} + \frac{\partial v_x}{\partial r}\right)\right] + \left(\frac{1}{r}\right)\frac{\partial}{\partial \theta}\left\{\mu\left[\left(\frac{1}{r}\right)\frac{\partial v_x}{\partial \theta} + \frac{\partial v_\theta}{\partial x}\right]\right\} . \qquad (6)$$

In the three previous equations, $\mu = \mu(T)$ is the viscosity and

$$\operatorname{div}\vec{v}_v = r^{-1}\left[\frac{\partial(rv_r)}{\partial r} + \frac{\partial v_\theta}{\partial \theta}\right] + \frac{\partial v_x}{\partial x} .$$

In general, the viscosity is expressed by an empirical relation. The terms F_r, F_θ, and F_x are the r, θ, and x components of the body forces per unit volume. In the absence of body forces other than those due to gravity, the magnitude of the resultant of the three forces is $F = \rho g_a$, where g_a is the apparent acceleration of gravity. When the coordinate system is in motion, the apparent gravity may be much larger than the standard gravity, g. Consequently, the induced pressure gradient can be significantly large. With the above equations it can be shown that when the fluid is acted upon by the body force only, the ratio of the pressures at the two ends of a tube of length L is approximately

$$\frac{P_2}{P_1} \cong \exp\left(g_x R^{-1} T^{-1} L \sin \psi\right) ,$$

where

ψ is the angle between the longitudinal axis of the tube and a horizontal plane,

T is temperature,

R is the gas constant (for air, $R = 1716 \ ft^2/sec^2/^\circ Rankine$), and

g_x is the apparent (absolute) acceleration in the direction of the tube axis.

The effect of the body force can be large when the tube axis is parallel to the direction of motion. However, even when acceleration in that direction is 30 times the standard gravity, i.e., when $g_x = 30(32.174 \ ft/sec^2)$, the pressures at the ends of a 10-foot tube differ by only 1 percent if $T = 100^\circ F$. At higher temperatures, the differential pressure is correspondingly smaller. Thus, the effect of the body force, F, is normally small and will be neglected in Equations 4, 5, and 6.

There are now four equations (3 through 6) and five unknown quantities (p, T, v_r, v_θ, and v_x). The energy equation is the additional relation which is required to define the motion. However, if the flow process is iso-thermal, there are only four unknowns and the above equations are sufficient. Unfortunately, even with this

simplification there is no known method for general solution. The solution is apparently possible with the aid of a computer, but further simplifications will be made to provide equations which are more manageable.

If $v_r = v_\theta = \partial v_x / \partial x = \partial v_x / \partial \theta = 0$, which implies a steady, fully developed, incompressible flow in a straight tube of constant diameter, then only the last of the three motion equations exists. It reduces to the following expression when the fluid viscosity is constant and the body force is zero

$$\frac{dp}{dx} = \mu \left[\frac{d^2 v_x}{dr^2} + \left(\frac{1}{r}\right) \frac{dv_x}{dr} \right] . \tag{7}$$

For the known boundary condition $v_x = 0$ when $r = r_o$, which requires that no slip flow occur at the walls and therefore implies a continuum, the solution to Equation 7 is

$$v_x = -\left(\frac{1}{4\mu}\right)\left(r_o^2 - r^2\right) \frac{dp}{dx} , \tag{8}$$

where the axial pressure gradient $dp/dx \equiv (p_2 - p_1)/L$, and p_1 and p_2 are constant pressures at either of the open ends of a tube of length L. The average velocity v is

$$v = \frac{1}{r_o^2} \int_0^{r_o} 2v_x r\, dr = -\left(\frac{r_o^2}{8\mu}\right)\frac{dp}{dx} . \tag{9}$$

This is the well-known Hagen-Poiseuille equation. A compressible flow will be approximated by applying the Hagen-Poiseuille expression to each increment of tube length. The average velocity becomes

$$v = -\left(\frac{r_o^2}{8\mu}\right)\frac{\partial p}{\partial x} , \tag{10}$$

and the average velocity gradient along the tube axis is

$$\frac{\partial v}{\partial x} = -\left(\frac{r_o^2}{8\mu}\right)\frac{\partial^2 p}{\partial x^2} . \tag{11}$$

By assuming a quasi-steady flow and substituting Equations 10 and 11 into Equation 3, the following relation is obtained

$$\frac{\partial p}{\partial t} - \left(\frac{p}{T}\right)\frac{\partial T}{\partial t} + v_r \frac{\partial p}{\partial r} - \left(\frac{pv_r}{T}\right)\frac{\partial T}{\partial r} + p\frac{\partial v_r}{\partial r} + \left(\frac{v_\theta}{r}\right)\frac{\partial p}{\partial \theta} - \left(\frac{pv_\theta}{rT}\right)\frac{\partial T}{\partial \theta} + \left(\frac{p}{r}\right)\frac{\partial v_\theta}{\partial \theta} - $$

$$\left(\frac{r_o^2}{8\mu}\right)\left[\left(\frac{\partial p}{\partial x}\right)^2 - \left(\frac{p}{T}\right)\frac{\partial p}{\partial x}\frac{\partial T}{\partial x} + p\frac{\partial^2 p}{\partial x^2}\right] + \frac{pv_r}{r} = 0 . \tag{12}$$

10

Consistent with the initial assumptions of an isothermal, fully developed flow, the terms v_r, $\partial T/\partial t$, $\partial T/\partial x$, and all derivatives with respect to r and θ are zero. Equation 12 then reduces to the following second-order, non-linear equation

$$\frac{\partial p}{\partial t} = \left(\frac{d^2}{64\mu}\right)\frac{\partial^2 (p^2)}{\partial x^2} ,$$ (13)

where d is the tube diameter.

In general, the boundary and initial conditions for a tube which has the closed end at x = L are

(i) $p(0, t) = f(t)$,

(ii) $p(x, 0) = f(0)$, and

(iii) $\frac{\partial p}{\partial x}(L, t) = 0$.

The first boundary condition is the forcing or driving function and states that the pressure at the open end (x = 0) of the tube is a specified function of time. This may be the unknown function in some problems and, in that event, Equation i may be replaced by the known function $p(L, t) = g(t)$. Equation ii states that the pressure is initially constant throughout the tube. The last boundary condition is derived from Equation 10 by specifying that velocity at the closed end of the tube is zero. This, of course, implies negligible volume in the reservoir.

Equation 13 may be made dimensionless by defining a pressure coefficient $P = p/p_o$, a length $X = x/L$, and a time $r = t/t^*$, where p_o is a constant reference pressure, L is the tube length, and t^* is a positive increment of time. The final equation, with a change in notation, is

$$P_r = KP^2_{XX} ,$$ (14)

where the dimensionless coefficient $K = (p_o t^* d^2)/(64\mu L^2)$. The corresponding boundary and initial conditions for the response equation (Equation 14) are

(iv) $P(0, r) = F(r)$,

(v) $P(X, 0) = F(0)$, and

(vi) $P_X(1, r) = 0$,

where the dimensionless functions are $F(r) = p_o^{-1}f(t)$, $F(0) = p_o^{-1}f(0)$, and $P_X(1, r) = Lp_o^{-1}p_x(L, t)$.

Results

Equation 14 is similar in form to the nonsteady, one-dimensional diffusion equation. However, unlike the diffusion equation, the dependent variable is squared on the right-hand side of the pressure-response equation.

Although no general analytical solution to the response equation has been found, numerical solutions were obtained with an analog computer. The solutions relate the pressure coefficients at the two ends of the tube in the form of a ratio P_2/P_1 where the subscripts 1 and 2 refer to the open (X = 0) and closed (X = 1) ends, respectively. The ratio of the pressure coefficients reduces to the pressure ratio across the tube since the constant reference pressures p_o in the denominators of the coefficients cancel each other. Thus, $P_2/P_1 = p_2/p_1$ where p_2 is the pressure at the closed end of the tube and p_1 is the pressure at the orifice (open end).

Three forms of the general forcing function $F(r) \equiv P_1$, which is used in the boundary and initial conditions (Equations iv and v), were considered: step functions, ramp (linear) functions, and the conditions that correspond to constant-velocity flight in an isothermal atmosphere. The calculations were made for conditions that represent gas flowing both out of and into the tube with the pressure ratio varying from $0.5 \leq p_2/p_1 \leq 1.4$, approximately.

For a step function, the forcing function becomes $F(r) = 1$ when $r > 0$ and $F(r) = \overline{P}_1$ when $r \leq 0$. The constant pressure coefficient $\overline{P}_1$ is $\overline{P}_1 = \overline{p}_1/p_o$ where $\overline{p}_1$ and p_o are respectively the initial $(r \leq 0)$ and final $(r > 0)$ pressures at the tube inlet (X = 0). Figure 1 summarizes the results of the calculations. Ten step sizes were taken over the pressure ratio range $0.5 \leq p_2/p_1 \leq 1.5$. The pressure ratio is plotted as a function of the dimensionless time parameter $Kr = (p_o d^2 t)/64\mu L^2)$ where the reference pressure p_o is, as stated above, the final pressure in the tube, d is the tube diameter, t is time, μ is the viscosity coefficient, and L is the length of the tube. The results reveal that the time required for the pressures at the tube extremities to become essentially equal is nearly independent of the initial differential pressure, i.e., the size of the step. Further, for a given initial differential pressure and a given final pressure, the direction of flow in the tube does not measurably affect the time history of differential pressure $(p_1 - p_2)$.

For a ramp function, the forcing function is $F(r) \equiv P_1 = 1 + Ar$ where A is an arbitrary constant. The pressure coefficient is $P_1 = p_1/p_o$ where $p_1 = p_o\left[1 + (A/t*)t\right]$ and p_o is now defined as the initial $(r = 0)$ pressure in the tube. Figure 2 shows the results of the calculations when the pressure decreases with time. For convenience, the value of A was selected as A = -5. The pressure ratio across the tube is plotted versus dimensionless time $r = t/t*$, and various curves which represent different values of the parameter $K = (p_o t* d^2)/(64\mu L^2)$ are shown. With any initial pressure p_o, the pressure ratio across the tube continually increases as time increases. Figure 3 is a plot of the same parameters used in Figure 2, but corresponds to the case where the pressure at the open end of the tube increases; $p_1 = p_o\left[1 + (A/t*)t\right]$ where, in the calculations, A = 50. The results show that with any initial pressure, the pressure ratio across the tube first decreases and later increases.

In an isothermal atmosphere, the ambient pressure p_∞ at altitude h is $p_\infty = p_{SL} \exp (-gR^{-1}T_\infty^{-1}h)$ where g is the gravity constant, R is the gas constant, T_∞ is the atmospheric temperature, and p_{SL} is the atmospheric pressure at sea level. When a vehicle is ascending in an isothermal atmosphere at a constant velocity $\overline{V}$, the pressure p at any time t and any point on the vehicle is approximately $p = np_{SL} \exp (-gR^{-1}T_\infty^{-1}\overline{V}t \sin \emptyset)$ where n is a known constant and $\emptyset$ is the flight path angle with respect to a horizontal plane. If the open end of the tube is connected to an orifice on the vehicle surface, then $p = p_1$ and the pressure coefficient P_1 becomes $P_1 = p_1/p_o = \exp \left[(-gR^{-1}T_\infty^{-1}h*)\right]$ where the reference altitude $h* = \overline{V}t* \sin \emptyset$. For convenience the reference pressure is taken to be the initial (t = 0 and therefore h = 0) pressure in the tube; thus $p_o = np_{SL}$. Hence, the forcing function becomes $F(r) \equiv P_1 = \exp (-Cr)$ where the constant coefficient is $C = gR^{-1}T_\infty^{-1}\overline{V}t* \sin \emptyset$. Similarly, it can be shown that when the vehicle is descending at a constant velocity from an altitude h*, the forcing
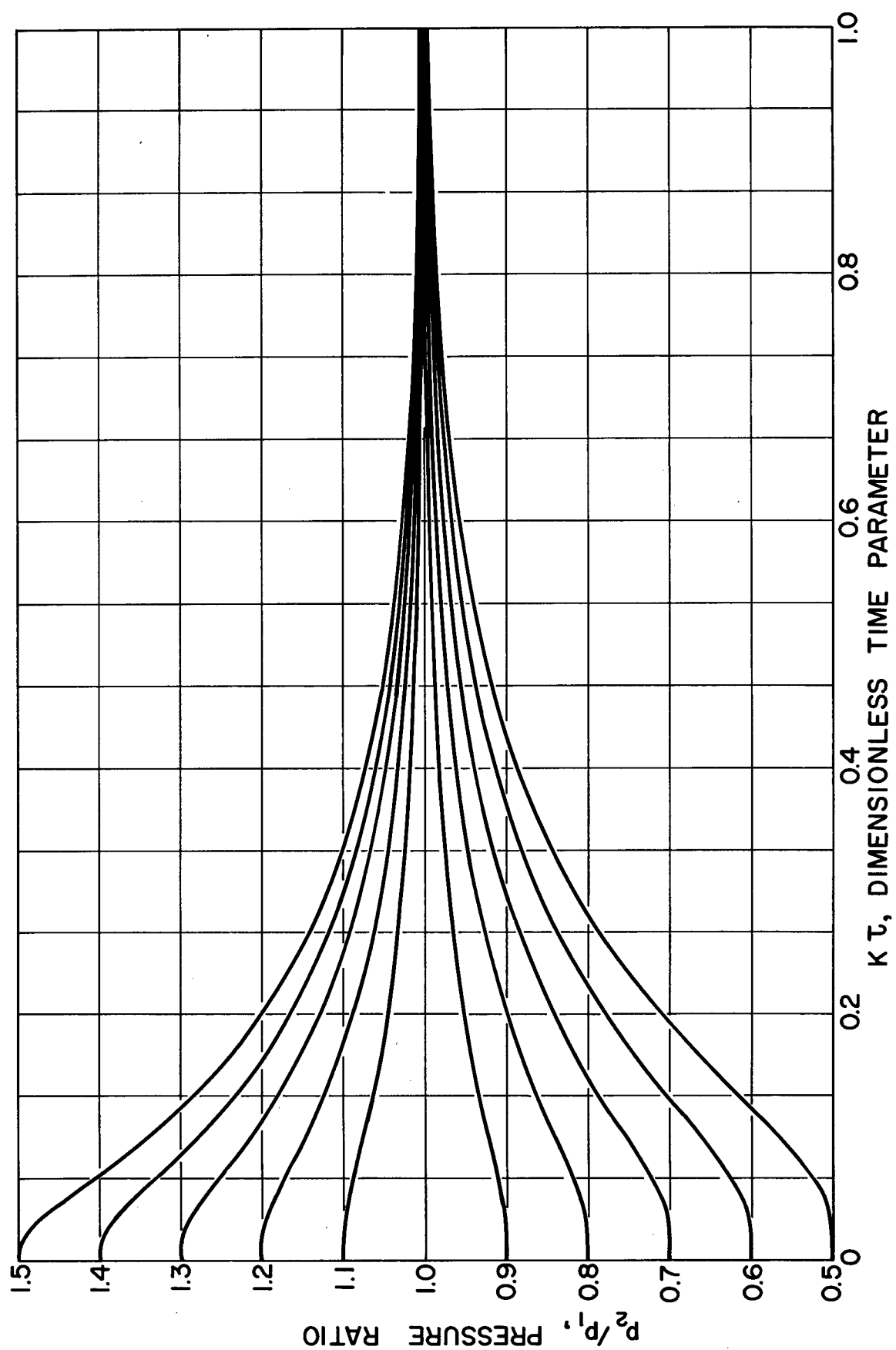
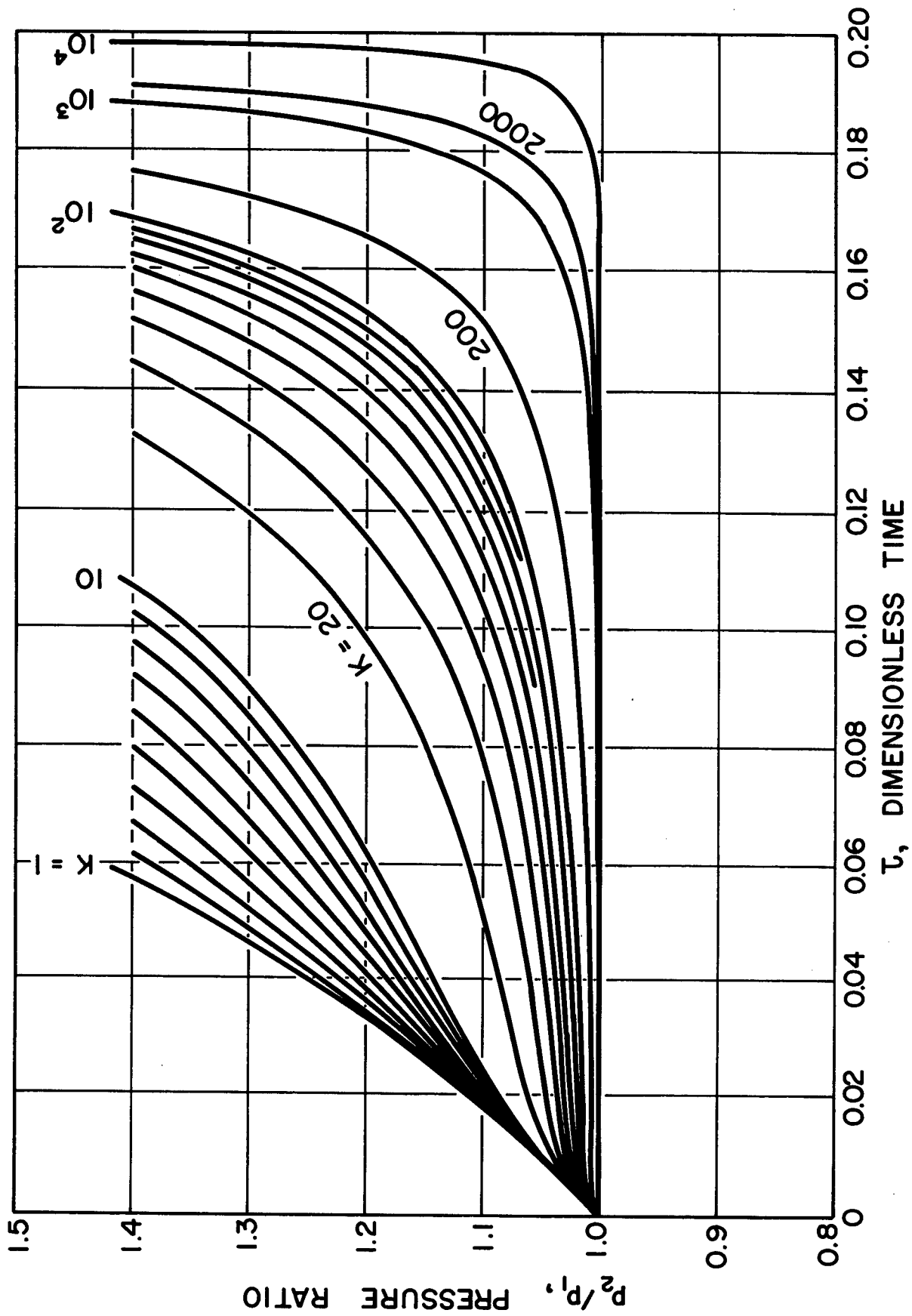Figure 1. Pressure Response to Step Forcing Functions of Various Sizes

13

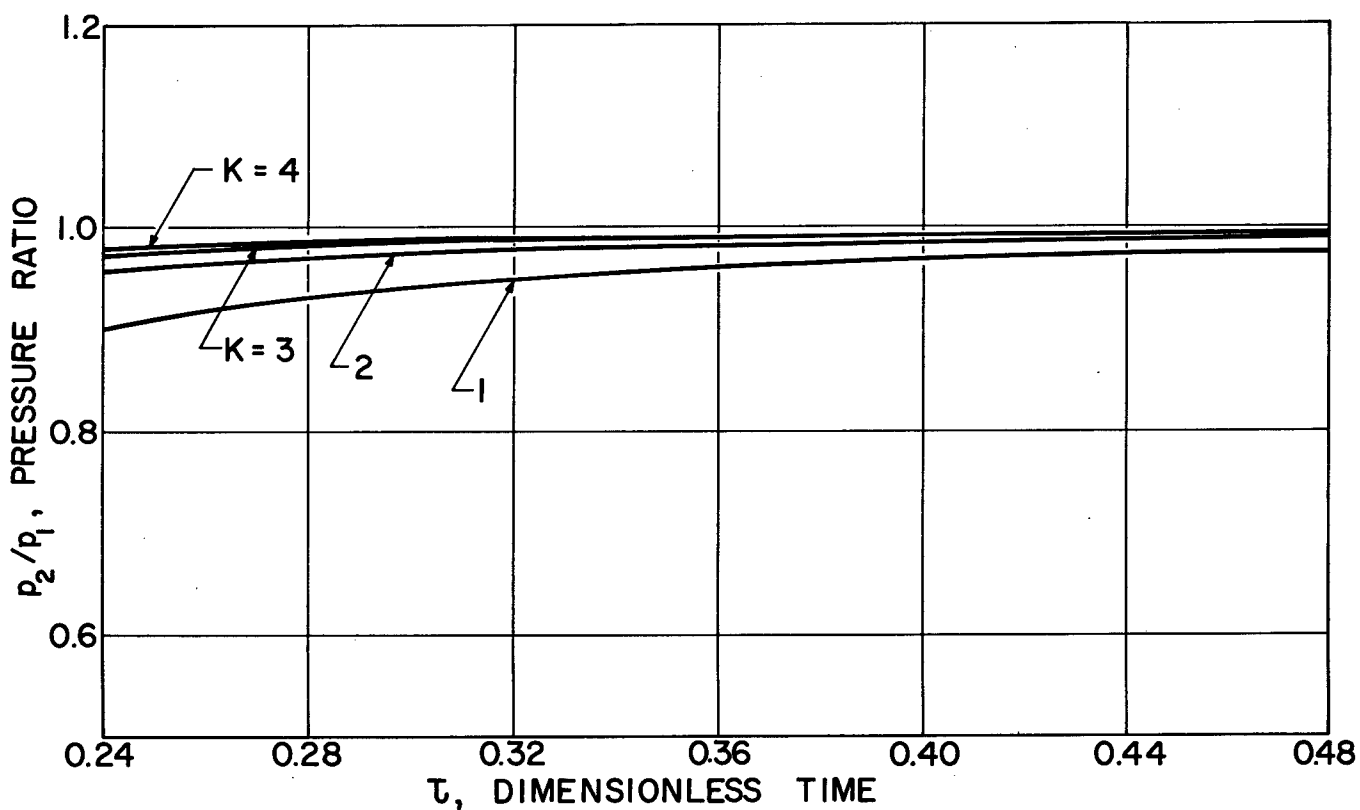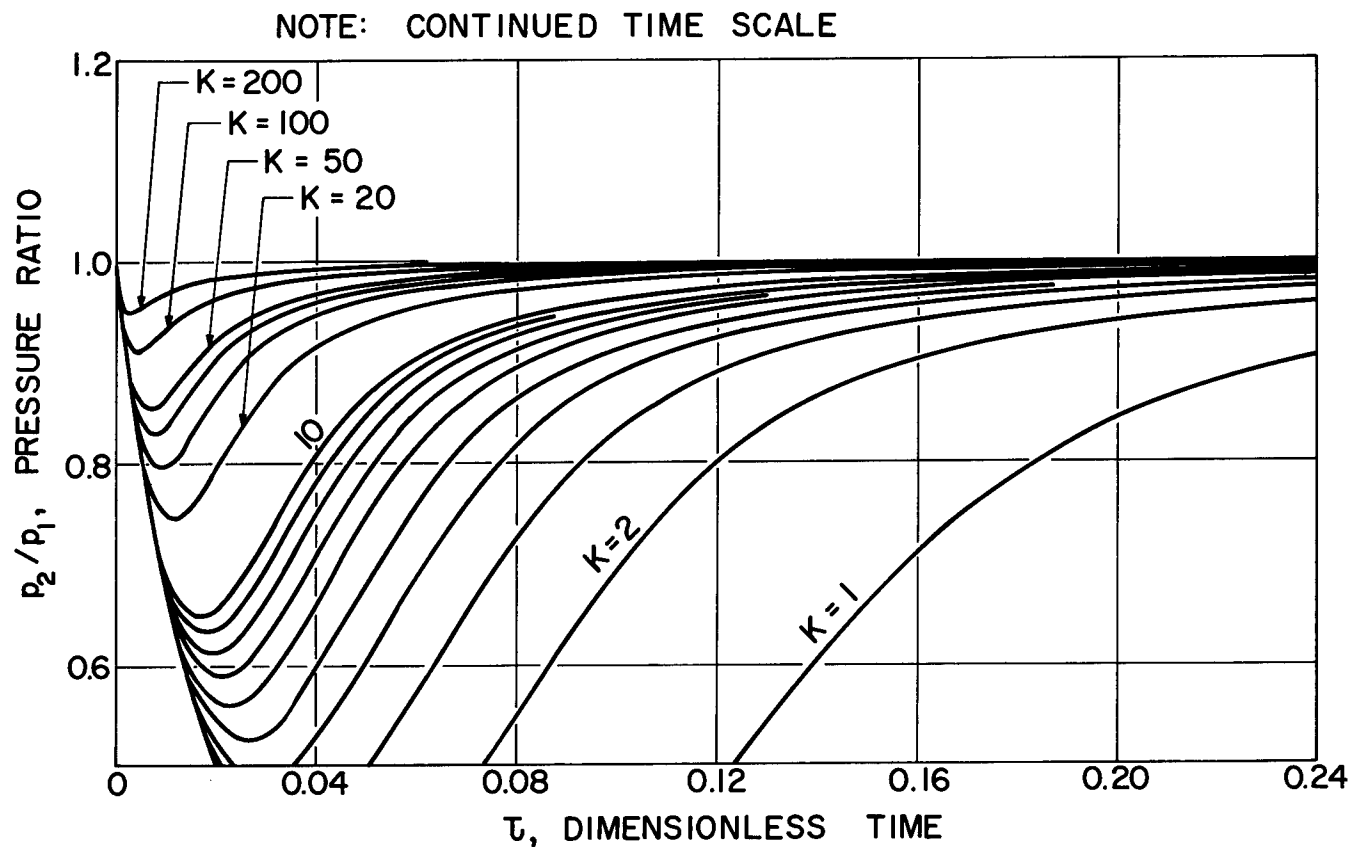Figure 2. Pressure Response to Linear Forcing Functions (Decreasing Pressure)

14

Figure 3. Pressure Response to Linear Forcing Functions (Increasing Pressure)

function is $F(r) \equiv P_1 = \exp(Cr)$ where, again, the reference pressure is the initial ($t = 0$ and $h = h^*$) pressure in the tube; i.e., $p_o = np_{SL} \exp(-C)$. For both the ascending and descending flight conditions, the constant C has been taken as 10 in the calculations. At normal pressures and temperatures, this value corresponds to an altitude range from sea level to a maximum of several hundred-thousand feet.

Figure 4 shows the solution to Equation 14 with the boundary condition $F(r) = \exp(-Cr)$ and the initial condition $F(0) = 1$. The pressure ratio p_2/p_1 is plotted as a function of a dimensionless time $r + r_o = (t/t^*) + r_o$, and various curves are shown which represent arbitrary values of the parameter $K = (p_o t^* d^2)/64\mu L^2)$. A sliding time scale is used with each curve since, after an initial transient phase, an approximate steady-state solution exists which is common to all values of K. The origin for each of the response curves is displaced by an amount r_o which depends only on the value of K, and is indicated at several places in Figure 4. The value of r_o is approximately defined by the relation $10r_o \cong -\ln(K/10^3)$. In the ascending flight condition, pressure ratio first increases at a rapid rate, and, after the transient phase, the rate of increase becomes relatively small ($K \gg 1$). However, the pressure ratio continues to increase as altitude (time) increases. The solutions to the response equation indicate that even if the tube is short and the flight velocity is low, eventually an altitude will be reached above which the pressure ratio will exceed an arbitrary value. Of course, the mean-free path of the gas in the tube normally decreases with altitude, and when that dimension becomes comparable with the tube diameter, the continuum concept is no longer satisfactory. The criterion for this limitation is considered later in the "Discussion" section.

Note that the application of the results is not limited to values of the parameter K less than 10^3 which is the maximum value shown in Figure 4. If $K > 10^3$, then $r_o < 0$, and the pressure ratio is approximately unity during the time interval $0 \leq r < |r_o|$. In this time interval, the pressure ratio or differential pressure cannot be determined without cross plotting and extrapolating the calculations. When $r > |r_o|$, the existing data are sufficient to determine pressure response.

Figure 5 shows the solution to Equation 14 with the descending-flight boundary conditions; $F(r) = \exp(Cr)$ where $C = 10$, and $F(0) = 1$. As in the previous figure, a sliding time scale is used with each curve. The pressure ratio is plotted versus the dimensionless time $r + r_o$ where r_o is approximately defined by the relation $10r_o \cong \ln(2K)$. The results are similar to those corresponding to the ascending flight conditions in that, after the transient phase, an approximate steady-state solution exists which is common to all values of the parameter K. Thus, these data may be used to determine the pressure response of a measuring system in a vehicle which is within the applicable altitude range, even though the vehicle may have descended from higher altitudes where the continuum concept is not necessarily valid or where the initial condition differs from that used in the calculations.

The results that are shown in Figures 4 and 5 may be used to determine the approximate pressure response of sensing systems in real atmospheres. This requires iteration since the constant K is variable in a real atmosphere. The reference pressure p_o, which is used in the calculation of K, will be a fictitious initial pressure calculated for an isothermal atmosphere of temperature T_∞, but reduces to a true pressure in the real atmosphere at the desired altitude. If the vehicle is accelerating or decelerating as will be the case with general trajectories, the pressure coefficient C_P will be a variable and n will not be constant. This effect may be taken into account by dividing the flight path into parts that are approximately constant-velocity intervals, and applying the calculating procedure to each interval.
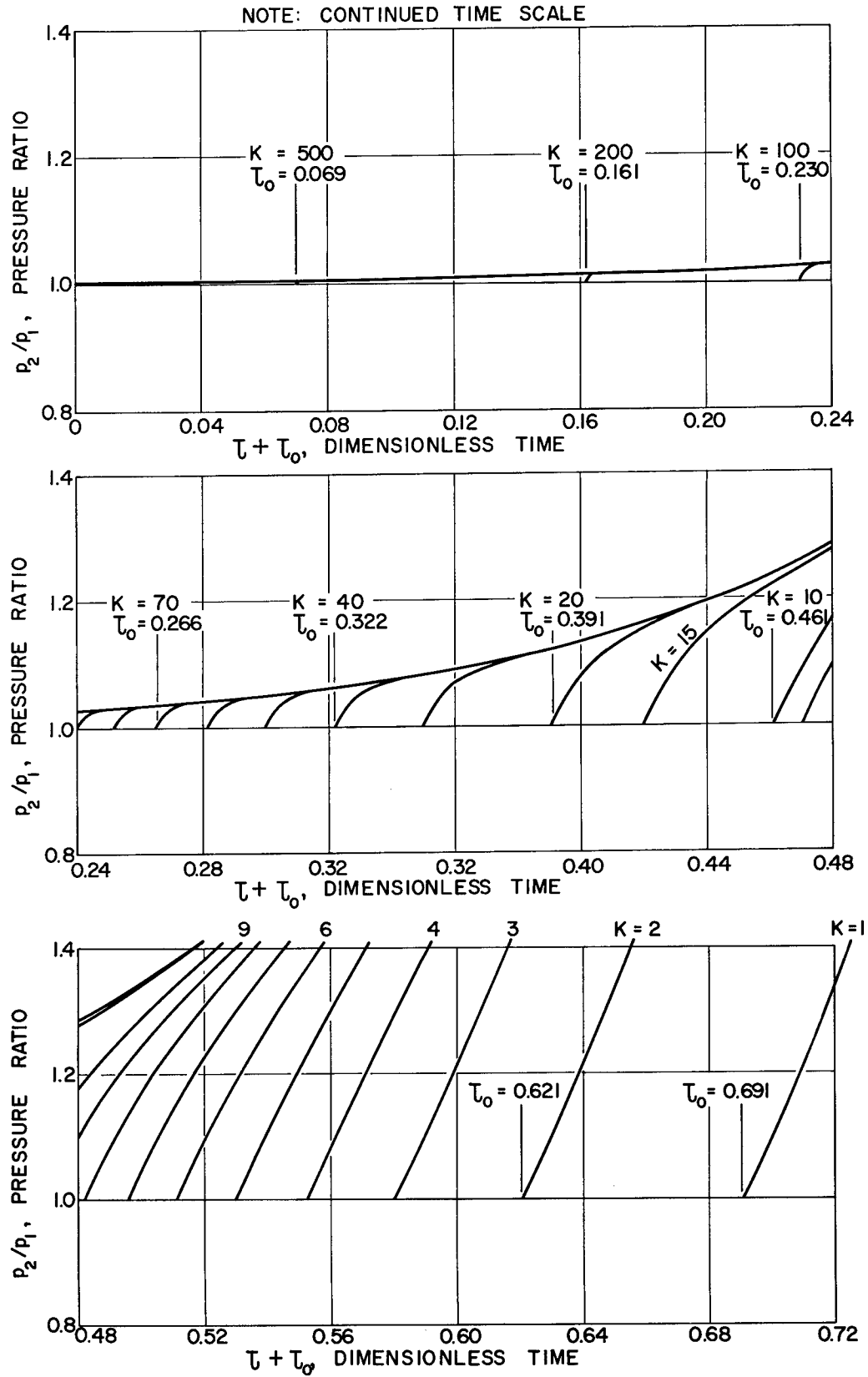
Figure 4. Pressure Response During Ascending Flight in Isothermal Atmospheres
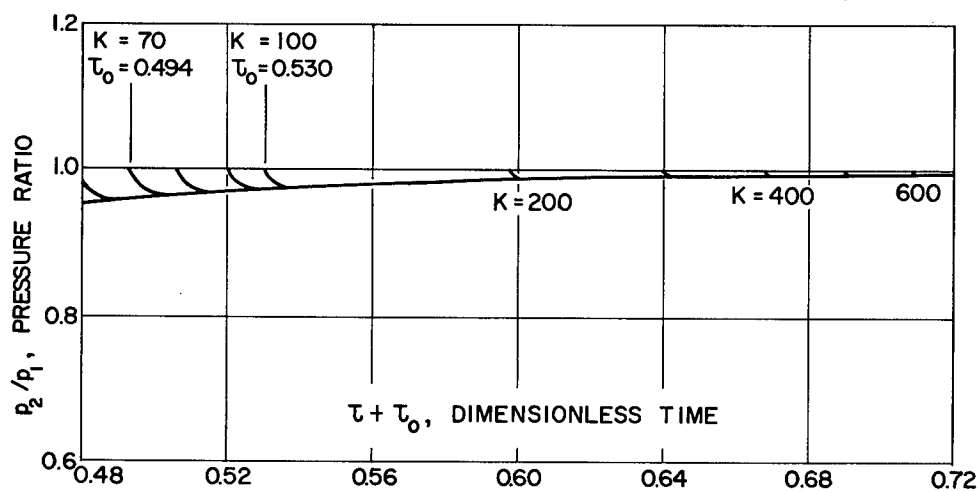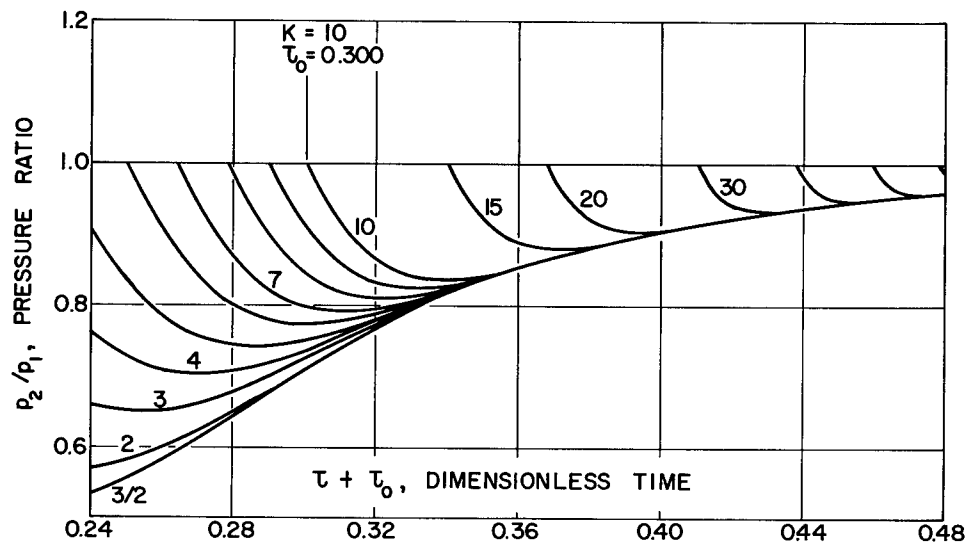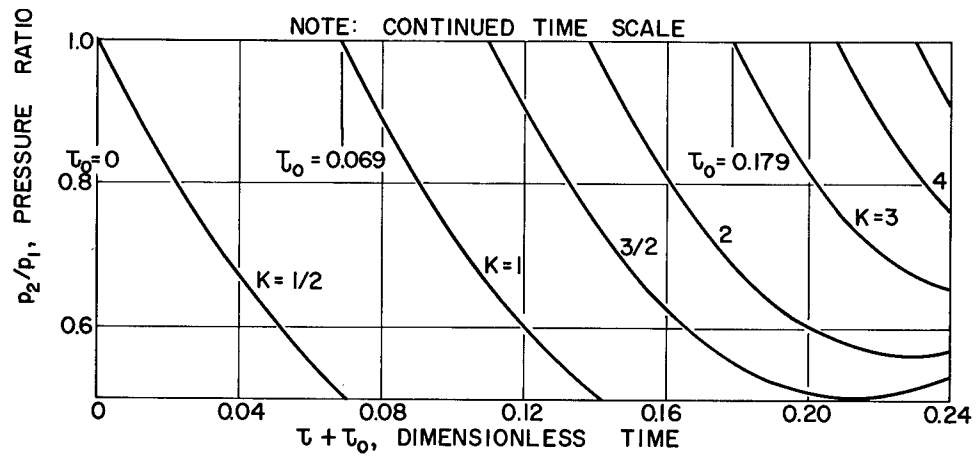
17

Figure 5.   Pressure Response During Descending Flight in Isothermal Atmospheres

<center>Discussion</center>

As indicated previously, the analysis is applicable only when the Knudsen number is much less than unity. Thus, there is some small Reynolds number below which the the response equation is not valid. The mean-free path λ can be written $\lambda = kT_1/(\xi p_1 \pi \sigma^2)$, where k is Boltzmann's constant, T_1 is temperature, $\xi = 2^{1/2}$ if the velocity distribution is Maxwellian, and the product $\pi\sigma^2$ is the collision cross-sectional area for a rigid spherical molecule. If T_1 is measured in degrees Rankine and p_1 is pounds per square foot, the mean-free path of air becomes $\lambda \cong 8.88 \times 10^{-7}(T_1/p_1)$ feet. Since the dimensionless Knudsen number, λ/d, must be small compared with unity, then $8.88 \times 10^{-7}(T_1/p_1 d) \ll 1$. Therefore, the response equation is valid for flight conditions in the earth's atmosphere when $p_1 d/T_1 \gg 10^{-5}$, where p_1' is pressure in pounds per square foot, d is tube diameter in inches, and T_1 is temperature in degrees Rankine.

In actual flows, the radial distribution of velocity is not fully developed near the tube inlet. The length ℓ required to attain fully developed, laminar flow is a function of Reynolds number and is discussed in Schlicting (see Bibliography); the required length in a steady, laminar flow is approximately $\ell/d = 0.03 R_N$, where Reynolds number is based on tube diameter. Since in the analysis presented here a fully developed profile was assumed, it is implied that the tube length L is large compared with the dimension ℓ. Therefore, the response equation is limited to the geometry range $L/d \gg 0.03 R_N$.

Shapiro (see Bibliography) shows that there is a limiting Mach number M for continuous isothermal flow in a tube. The magnitude of the limiting Mach number in a steady flow is $M = \gamma^{-1/2}$, where γ is the ratio of specific heats. When a subsonic, isothermal flow approaches the limiting condition, choking effects occur and fluid properties vary rapidly. It is expected that the response equation will not describe the pressure distribution accurately near the limiting condition, since, in this analysis, the possibility of large variations in fluid properties was precluded. Further, Shapiro shows that to maintain isothermal flow at the limiting condition, an infinite heat-transfer rate is required. Hence, the basic assumption of isothermal flow is not realistic when $M \to \gamma^{-1/2}$. The application of the results presented in Figures 1 through 5 should be therefore limited to the corresponding pressure-ratio range.

No experiments have been made and there are no available data to compare with the analytical results. However, when the flow is steady, the response equation can be integrated to define the axial pressure distribution, and a comparison can be made with existing experimental data. This comparison will provide an indication of the accuracy of the response equation.

If the flow is steady, then $P_\tau = 0$, and Equation 14 reduces to the following differential equation

$$P^2_{XX} = 0 . \tag{15}$$

With the two boundary conditions

(vii) $P(0) = P_1$,

(viii) $P(1) = P_2$,

<center>19</center>

Equation 15 can be easily integrated. The result is

$$P/P_1 = \left\{ 1 + \left[(P_2/P_1)^2 - 1 \right] X \right\}^{1/2} , \tag{16}$$

where $P = P(X)$, $P_2/P_1 \leq 1$, and $X = x/L$. Since the pressure coefficient is based on a constant reference pressure, Equation 16 reduces to

$$p/p_1 = 1 + \left[(p_2/p_1)^2 - 1 \right] \left[x/L \right]^{1/2} , \tag{17}$$

where p_1 and p_2 are respectively the inlet ($x = 0$) and exit ($x = L$) pressures. This relation describes the axial, static pressure distribution in a constant-diameter tube and it pertains to laminar, isothermal flow of a compressible fluid.

Equation 17 can be also derived from steady-flow considerations. That type of derivation is reported in Ducoffe's study (see Bibliography) and the equation is compared with the results of experiments using air. In the experiments, exit pressure was approximately equal to ambient pressure at sea level. Consequently, the Reynolds number is large; the maximum Reynolds number, based on tube diameter, is of order 10^6. The pressure ratio p/p_1 is plotted as a function of axial station in Figures 6 and 7, and a comparison is made of the experimental data with Equation 17. In Figure 6, which pertains to a tube with a length-diameter ratio of 667, the experimental data and the theoretical estimate differ by a few percent. In Figure 7, which corresponds to a length-diameter ratio of 229, the agreement is within a few percent only when the pressure ratio is approximately unity. Equation 17 and experimental data are in best agreement when the length-diameter ratio of the tube is large and the Reynolds number is small ($R_N < 2000$).

Conclusion

An equation is derived that approximately describes pressure response in a system that consists of a long tube connected to a reservoir of negligible volume. The equation pertains to the laminar flow of a compressible fluid in a constant-diameter tube and is applicable in the continuum regime. Numerical solutions of the equation are presented for three types of boundary conditions: step functions, ramp functions, and the functions that represent ascent and descent flight at constant velocity in an isothermal atmosphere. These solutions may be used to estimate the pressure ratio or differential pressure across the tube during transient conditions of flight in real atmospheres. They may also be used to determine the response of systems subjected to impulse pressure functions.
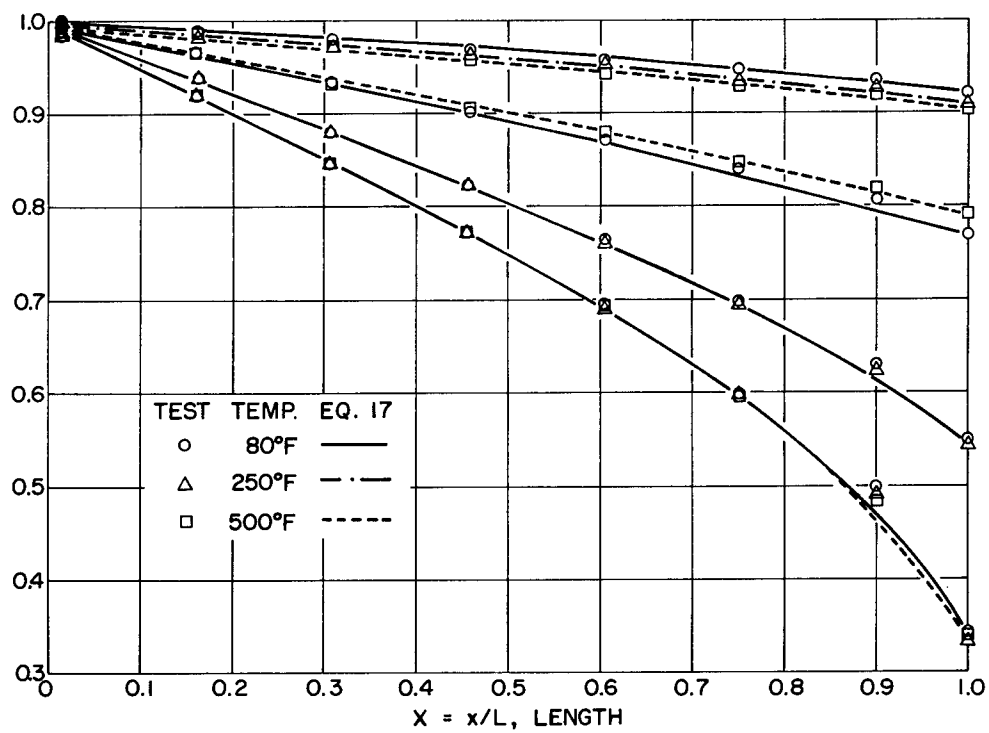
Figure 6. Comparison of Equation 17 with Experimental Data from
Small Tubes (d = 0.180 in, L = 10 ft)

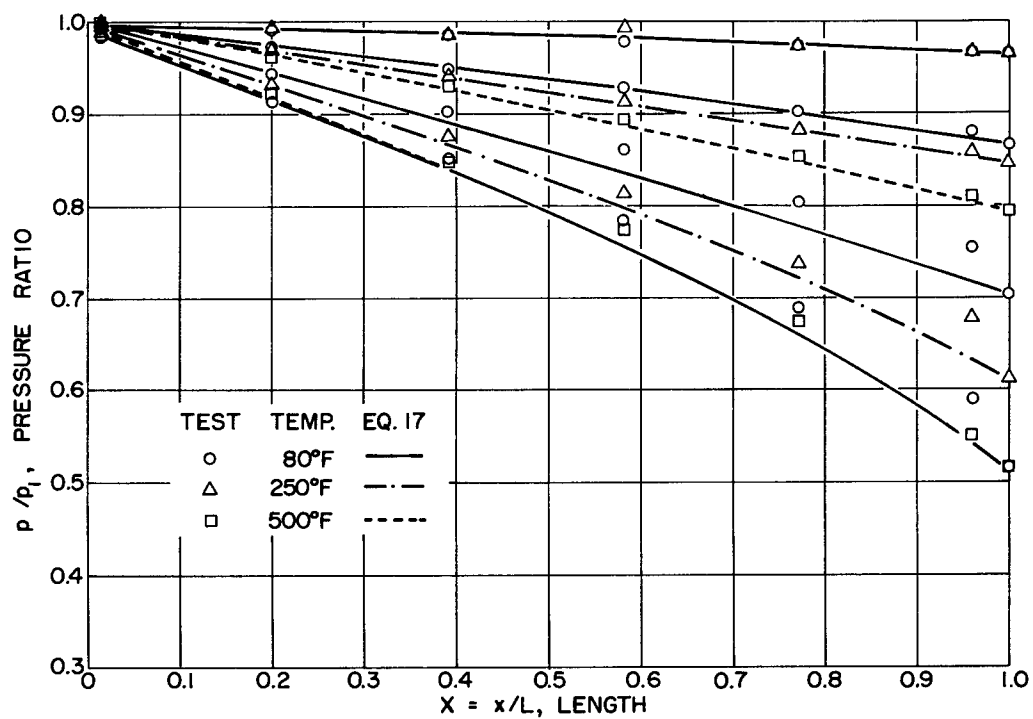Figure 7. Comparison of Equation 17 with Experimental Data from
Large Tubes (d = 0.524 in, L = 10 ft)

BIBLIOGRAPHY

Davis, W. T., Lag in Pressure Systems at Extremely Low Pressures, NASA TN 433r, September 1958.

Ducoffe, A. L., An Analytical and Experimental Investigation of Pressure Distribution and Pressure Drop in Small-Bore Tubing Using Air at Elevated Temperatures, Sandia Corporation SCTM 293-58(51), October 1958.

Ducoffe, A. L., and White, F. M., Jr., An Analysitcl and Experimental Investigation of Steady and Unsteady Flow in Tubing with Special Application to Simulated Missile Pressure-Sensing Systems, Sandia Corporation SC-4544(RR), March 1961.

Schlichting, H., Boundary Layer Theory, McGraw-Hill Co., New York, 1960.

Shapiro, A. H., The Dynamics and Thermodynamics of Compressible Fluid Flow (Vol. I), Ronald Press Company, New York, 1953.

Vaughn, H. R., The Response Characteristics of Airplane and Missile Pressure Measuring Systems, Aeronautical Engineering Review, November 1955.

OTIE (325)

Agricultural and Mechanical College of Texas, Aero. Eng. Dept., College Station, Texas

Brown University, Aero. Eng. Dept., Providence 12, Rhode Island

California Institute of Technology, Guggenheim Aeronautical Laboratory, Pasadena, California

California Institute of Technology, Jet Propulsion Laboratory, 4800 Oak Grove Drive, Pasadena, California

Carnegie Institute of Technology, Mech. Eng. Dept., Pittsburgh, Pennsylvania

Case Institute of Technology, Mech. Eng. Dept., Cleveland, Ohio

Catholic University of America, Department of Physics, Washington 17, D. C.

Colorado State University, Mech. Eng. Dept., Fort Collins, Colorado

Cornell Aeronautical Laboratory, Inc., 4455 Genesee Street, Buffalo 21, New York

Cornell University, Aero. Eng. Dept., Ithaca, New York

Detroit University, Aero. Eng. Dept., Detroit, Michigan

Georgia Institute of Technology, Aero. Eng. Dept., Atlanta, Georgia

Harvard University, Dept. of Applied Physics and Eng. Science, Cambridge 38, Massachusetts

Iowa State College, Dept. of Aero. Eng., Ames, Iowa

Lehigh University, Physics Dept., Bethlehem, Pennsylvania

Louisiana State University and Agricultural and Mechanical College, Mech. Eng. Dept., Baton Rouge, Louisiana

Massachusetts Institute of Technology, Dept. of Aeronautics and Astronautics, Cambridge 39, Massachusetts

Massachusetts Institute of Technology, Naval Supersonic Laboratory, 560 Memorial Drive, Cambridge 39, Massachusetts

Mississippi State College, Aero. Eng. Dept., State College, Mississippi

Municipal University of Wichita, Aero. Eng. Dept., Wichita, Kansas

New Mexico State University, Mech. Eng. Dept., State College, New Mexico

New Mexico State University, Physical Sciences Laboratory, State College, New Mexico

New York University, Dept. of Aeronautics, New York 53, New York

North Carolina State College of Agriculture and Engineering, Mech. Eng. Dept., Raleigh, North Carolina

Northeastern University, Mech. Eng. Dept., Boston, Massachusetts

Northwestern University, Mech. Eng. Dept., Evanston, Illinois

Ohio State University, Aero. Eng. Dept., Columbus 10, Ohio

OTS (75)

Oklahoma State University, Mech. Eng. Dept., Stillwater, Oklahoma

Oregon State College, Mech. Eng. Dept., Corvallis, Oregon

Pennsylvania State College, Aero. Eng. Dept., State College, Pennsylvania

Polytechnic Institute of Brooklyn, Aerodynamic Laboratory, 527 Atlantic Avenue, Freeport, New York

Princeton University, Aeronautics Dept., Princeton, New Jersey

Princeton University, Gas Dynamics Laboratory, Princeton, New Jersey

Purdue University, School of Aero. Eng., Lafayette, Indiana

Rensselaer Polytechnic Institute, Aeronautics Department, Troy, New York

San Diego State College, Aero. Eng. Dept., San Diego, California

Southern Methodist University, Aero. Eng. Dept., Dallas, Texas

State College of Washington, Mech. Eng. Dept., Pullman, Washington

Stanford University, Dept. of Aero. Eng., Palo Alto, California

State University of Iowa, Institute of Hydraulic Research, Iowa City, Iowa

State University of Iowa, Mech. Eng. Dept., Iowa City, Iowa

Stevens Institute of Technology, Mech. Eng. Dept., Hoboken, New Jersey

Syracuse University, Mech. Eng. Dept., Syracuse, New York

The Johns Hopkins University, Applied Physics Laboratory, Silver Spring, Maryland

The Johns Hopkins University, Mechanics Dept., Baltimore 18, Maryland

University of Alabama, Dept. of Aero. Eng., University, Alabama

University of Arkansas, Mech. Eng. Dept., Fayetteville, Arkansas

University of California, Mech. Eng. Dept., Berkeley, California

University of California at Los Angeles, Mech. Eng. Dept., Los Angeles 24, California

University of California, Institute of Eng. Research, 1301 South 46th Street, Richmond, California

University of Southern California, Aero. Lab. Dept., Box 1001, Oxnard, California

University of Southern California, Engineering Center, 3518 University Avenue, Los Angeles 7, California

University of Cincinnati, Aero. Eng. Dept., Cincinnati, Ohio

University of Colorado, Aero. Eng. Dept., Boulder, Colorado

University of Florida, Aero. Eng. Dept., Gainesville, Florida

University of Idaho, Mech. Eng. Dept., Moscow, Idaho